Journal Pre-proofs

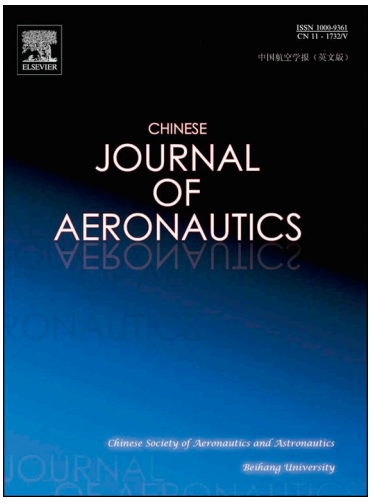

Characterisation of nonlinear response of 3D layer-to-layer angle interlock woven composites under warp tension

Shibo YAN, Junru LI, Mingming XU, Elena SITNIKOVA, Weiyi KONG, Shoufeng HU, Shuguang LI

PII: S1000-9361(25)00511-4
DOI: https://doi.org/10.1016/j.cja.2025.103905
Reference: CJA 103905

To appear in: *Chinese Journal of Aeronautics*

Received Date: 22 January 2025
Revised Date: 24 October 2025
Accepted Date: 24 October 2025

Please cite this article as: S. YAN, J. LI, M. XU, E. SITNIKOVA, W. KONG, S. HU, S. LI, Characterisation of nonlinear response of 3D layer-to-layer angle interlock woven composites under warp tension, *Chinese Journal of Aeronautics* (2025), doi: https://doi.org/10.1016/j.cja.2025.103905

Final Accepted Version

Contents lists available at ScienceDirect

Chinese Journal of Aeronautics

Journal homepage: www.elsevier.com/locate/cja

Characterisation of nonlinear response of 3D layer-to-layer angle interlock woven composites under warp tension

Shibo YAN [a,*], Junru LI[a], Mingming XU[b], Elena SITNIKOVA[c], Weiyi KONG[d], Shoufeng HU[e], Shuguang LI[f]

[a]*School of Aeronautic Science and Engineering, Beihang University, Beijing 100191, China*

[b]*School of Science, Harbin Institute of Technology (Shenzhen), Shenzhen 518055, China*

[c]*School of Engineering, Faculty of Engineering and Physical Sciences, University of Southampton, Southampton, SO17 1BJ, United Kingdom*

[d]*TaiHang Laboratory, Chengdu 610213, China*

[e]*AECC Commercial Aircraft Engine Co., LTD, Shanghai 200241, China*

[f]*Faculty of Engineering, University of Nottingham, Nottingham, NG7 2RD, United Kingdom*

Received 24 January 2025; revised 6 March 2025; accepted 26 May 2025

Abstract

3D woven composites, known for their exceptional structural integrity, are highly attractive for aeronautical applications, particularly in critical components such as aero-engine fan blades. Despite their promising potential, a comprehensive understanding of their mechanical behaviour remains essential for optimised design and application. Significant nonlinear behaviour well before the ultimate failure of 3D woven composites with a layer-to-layer angle interlock fibre architecture under warp tension has been observed in experiments. Although the same experimental observation for this type of material had been reported in the literature previously, the fundamental mechanisms of nonlinearity were not fully studied. In this work, the contributing factors that lead to this severe nonlinearity are

investigated and their effects on modelling the response of 3D woven composites are characterised. An appropriately defined mesoscale single-layer unit cell is adopted for this purpose to simplify the finite element modelling, along with a justification performed. Fibre tow/matrix debonding, damage in neat matrix and nonlinear shear in fibre tows have been identified as the most significant sources of nonlinearity and their modelling strategies are discussed. In comparison with the experiments, the results demonstrate the specific effects of each identified factor on the nonlinear behaviour of the material. As modelling of 3D woven composites is computationally costly, this study would provide important insights into the choice of appropriate modelling strategies for 3D woven composites in a design process.

Keywords: 3D woven composites, Nonlinearity, Mesoscale unit cell, Finite element modelling, Damage mechanisms, Warp tension

*Corresponding author. *E-mail address:* shiboyan@buaa.edu.cn (Shibo YAN)

1. Introduction[1]

3D woven composites offer superb integrity, making them an attractive candidate in aeronautic applications, particularly in aero-engine fan blades subject to impact and fatigue loading.[1, 2] Their integral construction in fibre architectures has eliminated a generic weakness of conventional laminated composites, where interlaminar interfaces are often exposed as initiation sites of damage.[3] The lack of appropriate reinforcement across the interfaces often allows the damage, once initiated, to propagate with little resistance leading to extensive delamination, which often compromise the structural integrity. In 3D woven composites, distinct features of interlaminar interfaces as singly connected surfaces in mathematical terms have been eliminated due to the presence of interlacing fibre tows in directions out of the plane of the material,[4] although this sometimes comes at a price of reduced in-plane performances.[5] On balance, a well-defined niche of potential applications can be identified. However, how such composites behave, and how they can be designed to provide the desired structural performances remains pretty much a virgin territory, with very little information, let alone any systematic guidelines, being available. Available knowledge is usually based on experimental observations and measurements on specific types of 3D woven composites, through which a wide variation in the mechanical behaviour resulting from different fibre architectures has been demonstrated for these materials.[6-12] This variation allows the scope for optimisation in the design of the material for a specific application, but it also presents

a significant challenge due to the lack of analysis tools in presence of a large number of possible weave patterns for these materials. In Ref. 13, an attempt has been made to parameterise the 3D woven composites so that their geometric constructions can be fully described in terms of a limited number of parameters. Although the number of parameters is substantially larger than what one would need for conventional laminates, given the sophisticated architectures one may have in general 3D woven preforms, it led a way forward to characterise such composites systematically, so that they would enter designers' vision during their materials selection process for a serious product development. Before this is fully established, persistent efforts will be required to build up the confidence based on the characterisation capability of such materials. The effective properties for linear elastic behaviour of such composites can be obtained through the use of an appropriate unit cell, as has also been illustrated in Ref. 13, where a Finite Element (FE) method based on unit cell modelling had been employed,[14] making the exercise substantially more demanding than for their laminated counterparts. However, this is currently the only means available which would deliver predictions with reasonably controllable accuracy.

3D woven composites tend to show characteristically different performances under loads in different directions,[8] indicating their strong anisotropy. In the meantime, they respond differently under tension and compression as soon as the magnitude of the deformation goes beyond the small deformation regime.[15, 16] What makes the behaviour of 3D woven composites more complex is that some of them show strong nonlinearity well before the ultimate strength of the materials under a specific direction. For instance, 3D woven layer-to-layer angle interlock composites, a typical type of 3D woven composites which involve more warp tow interlacing than others, were observed to be strong nonlinear under warp tension well before the ultimate strength of the materials.[8, 12, 17] As will be apparent, hardly any serious application can be contemplated for these materials if the stress and the strain levels have to be kept within the linear elastic regime, as their potential will be greatly underrated. Ignorance of the nonlinearity arising during the deformation process could misrepresent the performance of the material to such an extent that it would mislead or misinform serious applications.

The nonlinear behaviour of 3D woven composites can be caused by a number of factors, e.g. accumulation of damage in the constituent materials and interfaces, nonlinear constitutive law for constituent materials under large deformation, or their specific fibre architectures. It is still a challenging task to accurately predict the nonlinear behaviour due to their complex fibre architectures and damage behaviour, although some promising attempts have been reported based on mesoscale unit cell modelling for a variety of weaves,[18-25] or braids as another type of textile composites.[26-29] For 3D woven layer-to-layer angle interlock composites, though the improved interlacing level in fibre architectures is likely to further enhance the structure integrity, the nonlinear behaviour they showed is even more significant than their variations, such as 3D orthogonal woven composites. To systematically model the behaviour of such materials, all the possible sources that lead to the nonlinearity in the responses of the material should be identified and need to be properly accounted for in the adopted modelling strategies. This would complicate the models and increase modelling and computational costs. Sometimes, it is impossible to identify all the sources of nonlinearity due to the lack of understanding of the underlying mechanics of materials.

In order to provide a useful guidance to more systematic modelling in the future, it is the intention of this paper to investigate the contributing factors that lead to the nonlinearity on the behaviour of 3D woven composites and to offer their effective treatments. The parameters of a type of 3D woven composite with a layer-to-layer angle interlock weave pattern and relevant experimental results are introduced in Section 2. Severe nonlinearity was observed in the experimental stress-strain curves for this specific material under tension in the warp direction well before the ultimate failure. To characterise the nonlinear material behaviour, mesoscale finite element modelling is used, and the generation of the simplified unit cell model is described in Section 3. Modelling considerations have been made to different sources of nonlinearity in Section 4, namely, the debonding between the fibre tows and the matrix, damage in neat matrix and nonlinear shear in fibre tows, as well as a justification of the unit cell simplification on its thickness. The results are presented and discussed in Section 5.

2. Typical responses of a layer-to-layer angle interlock 3D woven composite to tensile loading

In layer-to-layer angle interlock 3D woven composites (also known as 2.5D woven composites in some studies[1]), there are distinctive differences in the geometry of the weft and the warp tows comprising the woven reinforcement. The former ones tend to be

generally straight, whilst the latter can have substantial undulations along their path. An example of a unit cell for woven textile composite of layer-to-layer angle interlock reinforcement architecture is shown in Fig. 1, illustrating differences in the warp and weft tow geometries.

The architectural differences have a substantial effect on the mechanical behaviour of the woven composites. In Ref. 17, coupon tests have been conducted on a range of composites, in which the woven preforms were all of layer-to-layer angle interlock configuration as shown in Fig. 1. The composites were made of 3D woven preform employing vacuum-assisted resin transfer moulding, details of which can be found in Ref. [30]. For the composites tested, distinctive behaviours in stress-strain responses under tension in the weft and warp directions have been observed as illustrated in Fig. 2.[17] The data shown are for composite with IM7 carbon fibre[31] reinforcement with Gurit PRIME™ 20LV epoxy as the matrix.[32] As can be seen in Fig. 2(a), under tension in the weft direction, stress-strain response remains nearly linear up to the point of failure. On the other hand, in the warp tension experiments, substantial reduction of tangential stiffness was observed as shown in Fig. 2(b), resulting in a nearly bi-linear appearance with a reasonably smooth transition knee.

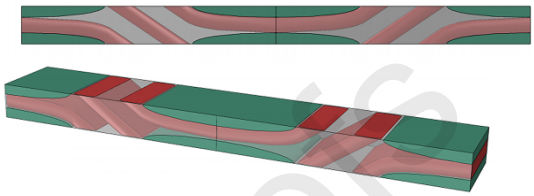

Fig. 1 Unit cell topology of a 3D woven composite with the layer-to-layer angle interlock reinforcement architecture, weft tows in green and warp tows in red.

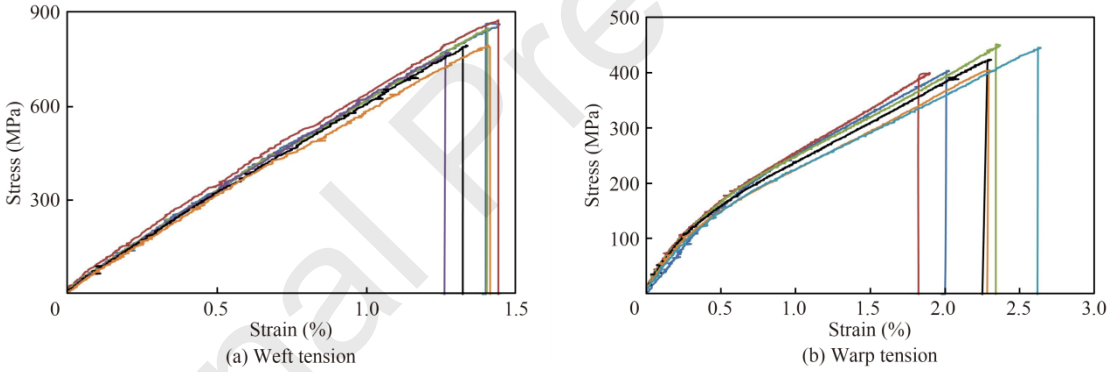

Fig. 2 Stress-strain curves under tensile loading in the weft and warp directions[17] (nonlinear behaviour well before the ultimate failure for warp direction is shown).

Whilst one would naturally expect that the undulations in the warp tows should undermine the material stiffness in the warp direction, the exact causes of the stiffness reduction are not obvious by large. Yet without understanding of the factors responsible for the stiffness reduction, one cannot consistently reproduce the realistic material behaviour theoretically, which in turn impedes the development of reliable numerical modelling techniques for such composites. Identification of such factors is the primary objective of the present paper.

3. Unit cell model and parameter definition

The approach adopted for the numerical analysis is based on Unit Cell (UC) modelling, which is the most common modelling technique for the woven textile composites, given the regular pattern of the interlocking architecture as present in these materials at the mesoscopic scale. The formulation of a unit cell involves primarily the derivation of the boundary conditions to be employed for the subsequent FE analysis of the unit cell. The derivation is based on the geometric translational symmetries, or periodicity, and sometimes the translations are not along a direction of any coordinate axis. Once properly formulated, these boundary conditions will involve average strains as the key degrees of freedom. By making correct use of these key degrees of freedom, the efforts of post-

processing of the FE results can be waived if one is interested only in the effective properties of the materials. To avoid duplicating the established contents, readers are referred to Ref. 14 for details in terms of the boundary conditions and the appropriate use of the key degrees of freedom.

Based on the UC theoretical framework established in Ref. 14, UCs for the woven composites have been parameterised, formulated and validated in Ref. 13. The UC shown in Fig. 1 was in fact generated according to the procedure established in Ref. 13. One of its distinctive features is that it accommodates a single warp tow, which makes the model more computationally efficient compared to its counterparts containing several warp tows. With such selection of the UCs, they are arranged within the plane of the composite in a staggered manner, which makes the boundary conditions a little more complicated than those involving only orthogonal translational symmetries.

In Ref. 13, three major groups of parameters were defined that were required for definition of the parameterised UC of woven textile composite. First one comprises five topological parameters, defining the relative arrangement of the warp and weft tows as well as path of the warp tows in the weave. For the UC as shown in Fig. 1, their values are n_{offset}=0, n_{step}=n_{skip}=1 and n_{steep}=n_{deep}=2. Another group are the geometric parameters of the weave, including the geometric dimensions of the tow cross-sections and the distance between the tows. For IM7 carbon fibre woven composite as is analysed in this paper, those were measured directly from the micro-CT images in Ref. 30, and the measured values are given in Table 1.[30] The final set of the parameters are the mechanical properties of the constituents, namely, the matrix and the fibre tows. These are listed in Table 2.[32] While the former were taken directly from the resin datasheet, the properties of the latter were calculated through a microscale material characterisation, where IM7 tows were considered as unidirectional composites. The characterisation was conducted with in-house software UnitCells[33], which carries out elastic material characterisation in an automated way. The intra-tow fibre volume fractions, $V_{f,}$ that are also specified in the table, were estimated in Ref. 30 for the given IM7 carbon fibre composite.

Table 1 Input geometric parameters for 3D woven composite coupons.

Geometric term	Warp tow (V_f=83.5%)	Weft tow ($V_{f,}$=71.5%)
Width [30] (mm)	1.26	2.63
Height [30] (mm)	0.243	0.34
Aspect ratio of the tow cross-section	0.05	0.92
Distance between the tows [30] (mm)	0.05	1.38

Table 2 Input material properties of constituents.

Computational term	Warp tow	Weft tow	Matrix[32]	
E_1 (GPa)	32.6	198.100	E (GPa)	3.5
E_2=E_3 (GPa)	13.365	10.641	v	0.35
G_{12}=G_{13} (GPa)	5.987	4.415		
G_{23} (GPa)	4.259	3.646		
v_{12}=v_{13}	0.290	0.297		
v_{23}	0.450	0.459		

Finite element modelling of the parameterised woven composite UC model has been automated via the use of the purpose-written Python script as described in Ref. 13. Therefore, the FE model of the UC was generated by simply entering the input parameters as specified above, while the geometric construction, meshing and imposition of the boundary conditions, which are the most demanding part of the UC FE modelling, were carried out automatically. The model was meshed with the tetrahedral elements of a typical mesh size of 0.06 mm. Note that when generating the FE model, the script automatically reduces the heights of the tows to 0.95 of their input values to allow small space between the tows, which facilitates the mesh generation in those regions.

4. Modelling strategies

In this section, a number of selected modelling strategies reflecting the mechanical behaviour of 3D woven composites in FE modelling will be introduced. Fibre tow/matrix debonding, damage in neat matrix and nonlinear shear in fibre tows have been identified as the most significant sources of nonlinearity, although other possible sources of nonlinearity also exist. The effects of each strategy on the nonlinear behaviour will be then investigated and discussed in the following section. In addition, the strategy for selecting unit cell topology in the thickness direction for characterising the properties of 3D woven composites is highlighted, and its effects will be evaluated. It should be noted that this work is to identify the contributing factors for the observed nonlinearity well before the ultimate failure, therefore

fibre tow failure is not considered as it is not the failure mode dominating the nonlinearity in the experiment.

4.1. Debonding modelling

Debonding damage, defined as the interface damage between the impregnated fibre tows and the neat matrix, is a common failure mode for some 3D woven composites under specific loading,[15, 34] especially in the cases where the interface between the fibre tows and the matrix is subjected to significant stresses. Debonding damage is usually in a progressive manner, and it is likely to introduce stiffness degradation whilst the composite is capable of carrying further loading. In the experimental work introduced earlier, extensive debonding was observed in the tested 3D woven specimens. Consequently, debonding modelling is considered as one of the essential modes of damage and major sources of nonlinearity. An appropriate modelling strategy has to be incorporated in order to capture its effects on the behaviour of 3D woven composites as is investigated in this paper.

The Cohesive Zone Model (CZM) as implemented in Abaqus has been successfully applied to the delamination problem in conventional laminates of unidirectional plies[3] and the debonding damage in 3D woven composites.[20] The formulation of the cohesive behaviour employed in this work correlates cohesive tractions in the normal, first shear and second shear directions (σ_n, τ_s, and τ_t) with their corresponding separations (δ_n, δ_s, and δ_t) through a bilinear constitutive law with a linear elastic and softening behaviour, which is geometrically the simplest form to implement. Results for global load-displacement response are relatively insensitive to the exact shape of the traction–separation curve, provided that the correct interfacial strength and fracture toughness are applied.[35] The stiffnesses before the peak load are denoted by k_n, k_s and k_t respectively. The difference between the work done by the tractions along with their corresponding separations and the recoverable energy represents the energy release rate, G_n, G_s and G_t, for each fracture mode.[36] Here the initiation of damage begins when the stress components meet a quadratic stress-based criterion,

$$\left(\frac{\langle \sigma_n \rangle}{\sigma_n^0}\right)^2 + \left(\frac{\tau_s}{\tau_s^0}\right)^2 + \left(\frac{\tau_t}{\tau_t^0}\right)^2 = 1 \tag{1}$$

where σ_n^0, τ_s^0 and τ_t^0 denote the damage initiation stress components in the normal, first shear and second shear directions for each of the single-mode fracture modes I, II and III, respectively; and the angle brackets <*> denote Macaulay operator which takes the value of its argument only when that value is positive. After damage initiation, there is a reduction in interface stiffness until a complete fracture of the interface occurs, based on the mixed mode power law for damage evolution,

$$\left(\frac{G_n}{G_n^c}\right)^p + \left(\frac{G_s}{G_s^c}\right)^p + \left(\frac{G_t}{G_t^c}\right)^p = 1 \tag{2}$$

where G_n^c, G_s^c, and G_t^c are the critical energy release rate values in the normal, first shear and second shear directions under each of the single-mode delamination modes, and p is the power in the criterion. Regarding the specific load case and composite fibre architecture in this study, the debonding is mode II dominated.

Two typical 3D implementations provided by Abaqus are the cohesive elements and the cohesive contact surfaces. As the cohesive surface method was shown to require more computational resources when the Abaqus Standard solver was used as investigated in Ref. 3, the zero-thickness cohesive element method has been adopted in the debonding analysis. The zero-thickness cohesive elements were generated after meshing the geometries of matrix and fibre tows via a Python script. An illustration of the cohesive element interface is shown in Fig. 3. It is noted that the zero-thickness cohesive elements share nodes with adjacent matrix and fibre tow elements, and therefore the meshes generated on the matrix and the fibre tows conform to ensure correct meshing of the cohesive interface.

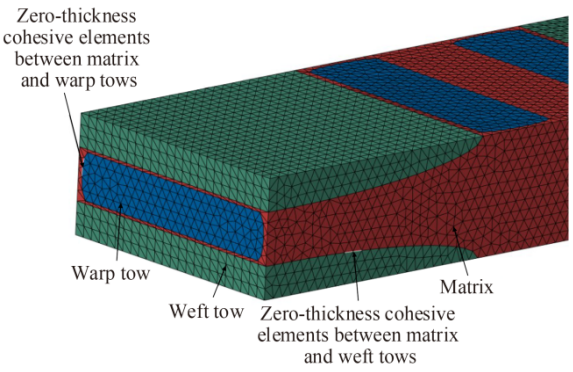

Fig. 3 Illustration of the zero-thickness cohesive element

interface between fibre tows and neat matrix in the unit cell model.

In the absence of experimental data for the interface properties in woven composites, the use of such data as found in the literature for generic carbon/epoxy interface was shown to be successful in predicting debonding damage.[20] The effects of cohesive parameters on structural performance have been discussed in detail in Refs. 20, 37, and therefore they will not be addressed in this paper. In the present study, the same cohesive properties will be inherited except a lower interfacial strength in shear (Table 3[20]), based on the outcomes of a parametric study conducted on this account with comparison to the experimental results as will be presented later.

Table 3 Parameters used for cohesive zone modelling.[20]

k_n=k_s=k_t	σ_n^0	τ_s^0	τ_t^0	G_n^c	G_s^c	G_t^c	p
(MPa/mm)	(MPa)			(mJ/mm^2)			
10^5	30	30	30	0.22	1.2	1.2	2

4.2. Damage in neat matrix

Besides resin in the impregnated fibre tows, there are also neat resin pockets in-between fibre tows in textile composites. Damage in the textile composites is likely to initiate in the neat matrix, the impregnated fibre tows or at their interfaces. Compared with typical damage in conventional laminates based on unidirectional (UD) plies, the neat matrix is a new phase specific for textile composites. Additional considerations, as well as computational resources, on matrix damage modelling will be needed in the finite element analysis of textile composites in order to represent this aspect of behaviour precisely, which is beyond the scope of the present paper.

The neat matrix can be considered as an isotropic material in modelling in contrast to an orthotropic material of the fibre tow. There are different failure modes for the matrix material under different loading, i.e.\ failure under tension, compression or shear. No established theoretical model comprehensive enough to incorporate all these effects is available. For the sake of simplicity, an isotropic elasto-plasticity model is adopted here to approximate the matrix damage as a compromise, because it is readily available in the commercial FE solver Abaqus. In this regard, the yield point is considered as the damage initiation, with the yield stress defined by the tensile strength of the matrix material. The Mises yield surface is used here, and a strain softening is introduced after the yield point to approximate the damage process of neat matrix as shown in Fig. 4. The initial yield stress is 70 MPa corresponding to an equivalent plastic strain of 0. As the equivalent plastic strain accumulates to 0.5, the yield stress decreases to 20 MPa. The underlying justification for the use of the plasticity model is to minimise the contribution to the tangential stiffness after the damage initiation.

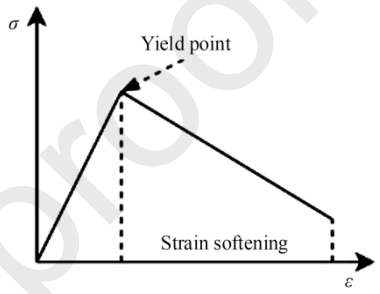

Fig. 4 Isotropic elasto-plasticity model used for neat matrix damage.

4.3. Nonlinear shear in fibre tows

Fibre tows in the woven composite concerned are conventionally regarded as a UD composite. Although a fibre tow undulates, the radius of curvature is many orders of magnitude greater than the fibre diameter. It is always reasonable enough to approximate a fibre tow as a UD composite of straight fibres when characterising it as a material. As a further approximation, it is assumed to be macroscopically homogeneous and transversely isotropic.

A characteristic of UD composites is their significant nonlinearity in the along-fibre shear stress-strain relationship. It is a well-known phenomenon, but it is usually presented in a pure shear stress state under a plane stress condition. It has been generalised to a 3D shear stress state in a rational manner in Ref. 38, where the objectivity has been observed. The nonlinear strain-stress relationship for a UD composite derived in Ref. 38 is given below,

$$\begin{cases} \gamma_{12} = a\tau_{12} + b\tau_{12}(\tau_{12}^2 + \tau_{13}^2) + c\tau_{12}(\tau_{12}^2 + \tau_{13}^2)^2 \\ \gamma_{13} = a\tau_{13} + b\tau_{13}(\tau_{12}^2 + \tau_{13}^2) + c\tau_{13}(\tau_{12}^2 + \tau_{13}^2)^2 \end{cases} \quad (3)$$

where a, b and c are three material constants to be determined in order to describe the nonlinear along-fibre shear strain-stress relationship.

This contribution[38] makes the consideration of nonlinear shear in fibre tows of 3D woven composites possible, which has often been ignored in the literature when modelling 3D woven composites. Therefore, the nonlinear along-fibre shear stress-strain model developed there has been adopted in the present analysis and implemented through a user defined material subroutine in Abaqus (UMAT). The results will be presented in the next section where the significance of the contributions the nonlinear shear behaviour makes will be demonstrated.

4.4. Unit cell simplification

3D woven composites have limited thickness, usually considerably smaller than their in-plane dimensions. As a result, the periodicity in the through-thickness direction is not always present. A simple example is an orthogonal weave in which the Z-binders go through from the top surface to the bottom surface and vice versa. Some layer-to-layer angle interlock weaves, such as the one investigated in this paper, exhibit periodicity locally in the thickness direction within the composite (excluding the surface layers). In such a case, using a single layer of the core for the unit cell can significantly simplify the unit cell model, albeit it introduces a degree of inaccuracy resulting from the negligence of the effects from the surface layers, which are of a different pattern from that of the core unit cell. The effects of this simplification on the predicted mechanical behaviour in terms of initial stiffness and damage will also be examined in this paper by comparing with the results from a whole-thickness unit cell as shown in Fig. 5. Its overall architecture is consistent with that of the composite tested in Ref. 17, namely, the latter had seven layers of weft tows through the thickness, and the structure of the surface layers was the same as shown in Fig. 5.

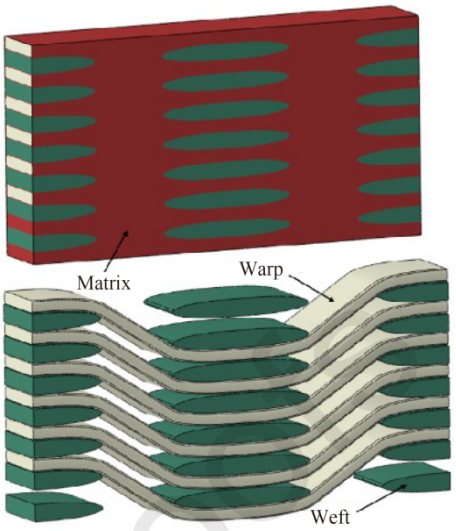

Fig. 5 A whole-thickness unit cell (fibre tows shown only in the bottom).

5. Results and discussion

A range of FE models were generated in Abaqus/CAE 2016, where the modelling strategies introduced in Section 4 were incorporated sequentially as listed in Table 4. A mesh convergence study for the CZM was performed and the converged global mesh size was found to be 0.06 mm, which is much smaller than the cohesive zone length to ensure there are sufficient cohesive elements to capture the stress distribution, i.e. approximately 0.3 to 1 mm as suggested by Cox and Yang[39] for aerospace carbon/epoxy interface. As a result, there are 396 512 elements and 84 513 degrees of freedoms in the single layer unit cell model including the zero-thickness cohesive elements. All the models as described in Table 4 were loaded via strain increments under a macroscopic stress state until the analyses aborted. Even so, sufficient knowledge has been obtained from the results, as will be presented and discussed below.

The 3D woven composite's responses to warp tension predicted for models described in Section 4 are compared with one another and also with the experimental results, in terms of initial stiffness, damage imitation and effective stress-strain curves. The predicted stress-strain curves for all models along with the experimental one are shown in Fig. 6.

It is obvious that all models analysed tend to overestimate the stress and the stiffness. However, the effects of the sources of nonlinearity considered make

different contributions to the predicted behaviour of the material. The single layer unit cell (denoted as SL) model with debonding damage alone overestimates the stiffness the most when compared to other models and the experiment. After introducing the debonding modelling, the stress-strain response is no longer linear, showing the trend of stiffness reduction (or hardening, in the conventional terminology of plasticity) similar to that of the experimental data. The stress-strain curve starts to deviate from its linear path approximately at a strain level of 0.35%, which is similar to that of the experimental curve. The debonding damage is one of the characteristic sources of nonlinearity involved in the stress-strain behaviour of the material concerned. Such debonding was clearly observed in the experiment, as can be seen in the microscopic images in Fig. 7 [40] showing damage in a specimen loaded to a stress level substantially below the expected final failure of the material. The adopted debonding modelling method seemed to capture the part of nonlinearity attributed to this mode of damage in 3D woven composites. At a macroscopic strain level similar to that of debonding damage initiation, the contours of damage over the interfaces between fibre tows and neat matrix are shown in Fig. 8. The location of these hot spots (full failure) seems generally agree with experimental observation in Fig. 7, although it should be noted that the idealised unit cell model was not able to account for the fibre tow contact from manufacturing.

Table 4 Unit cell models analysed and notation.

Model notation	UC type	Tow/matrix debonding	Matrix damage	Tow nonlinear shear
SL	Single layer	√	-	-
SL-M	Single layer	√	√	-
SL-N	Single layer	√	-	√
SL-MN	Single layer	√	√	√
WT	Whole thickness	√	√	√

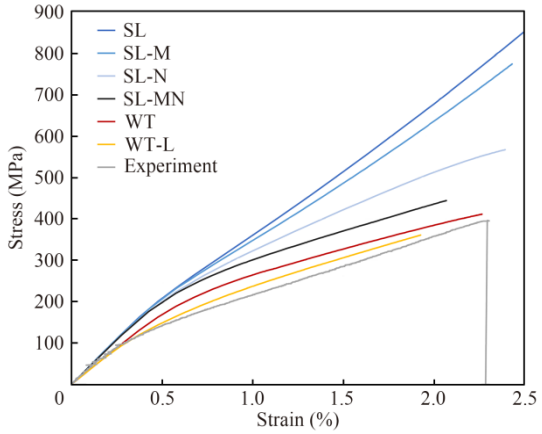

Fig. 6 Stress-strain responses from FE models and the experiment for the 3D woven composite in tension along the warp direction (WT with (15,15,15) MPa interface strengths denoted as WT-L).

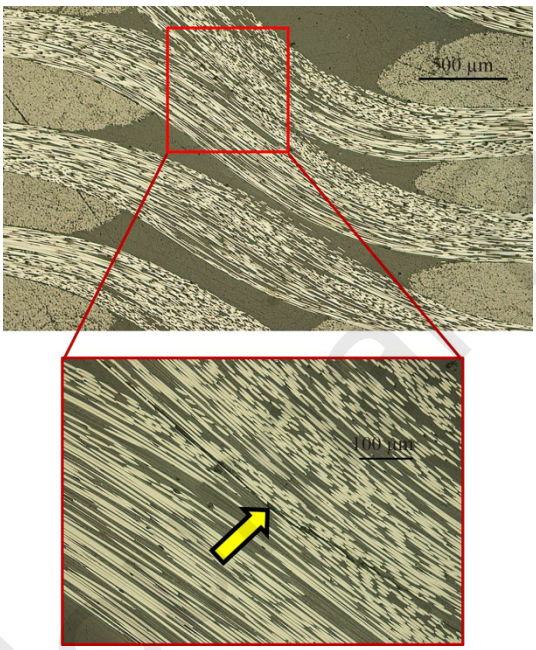

Fig. 7 Microscopic images showing initial debonding in the woven composite loaded to 0.35% strain in warp direction tension.[40]

At this load level, the stresses in some regions of the matrix in the model accounting only for damage associated with debonding have gone to levels much higher than the strength of the matrix material, which is 70 MPa for tensile strength of the epoxy resin. This suggests the need of a means of some kind to limit the stress carrying capacity of the neat matrix. By using the plasticity model to simulate matrix damage, the effect of this source of nonlinearity on the response of the material can be evaluated approximately. Comparing the stress-strain curve from the model incorporating both the debonding and the matrix plasticity (SL–M), with that from the debonding only model (SL), it is found as expected that the matrix damage would introduce further stiffness reduction after a certain load level. Although the number of elements reaching the yield stress is increasing rapidly (Fig. 9), the stiffness reduction that matrix damage causes is limited. This is because the warp tows bear more load than the matrix in this loading case.

Examining the stresses in the fibre tows, it can be found that some of the along fibre shear components reach rather high magnitudes, often considerably above the shear strength of the fibre tow as a UD composite (Fig. 10 (a)). It is well-known that UD composites exhibit significant nonlinearity in their along fibre shear behaviour, which is nevertheless typically neglected in terms of modelling. When nonlinear shear in fibre tows is incorporated in the modelling strategies, it leads to a significant stiffness reduction of the composite after loading to a strain level of 0.4%, where the nonlinear shear behaviour starts to take effect (Fig. 10 (b)). When the effects of the neat matrix damage and the nonlinear shear are considered separately, it can be seen from the predicted stress-strain curves as shown in Fig. 6 that the latter plays more significant role in degrading the stiffness of the material than the former does. A more practical scenario is that both take place in an analysis as is the case in reality. Although this does represent an improvement to the predicted results in comparison with the experimental data, there is still a significant gap between them. In particular, the initial stiffness of the material is unlikely to be affected by these sources of nonlinearity, because it is measured before the onset of the relevant mechanisms associated with these sources of nonlinearity. Something else must be responsible for the disparity in the initial stiffness.

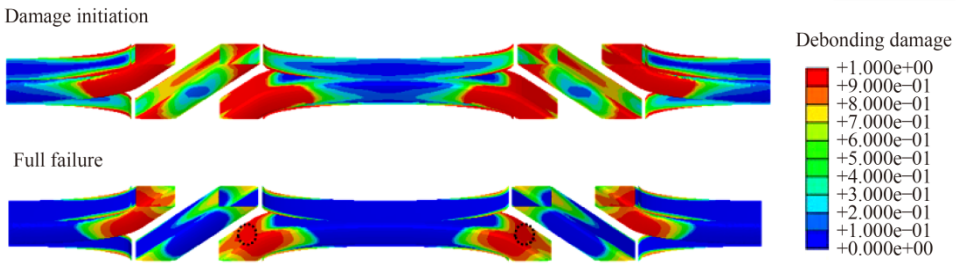

Fig. 8 Debonding damage (top: initiation; bottom: full failure) predicted by the single layer FE model (SL in Table 4) loaded to 0.357% strain in warp direction, showing interface only (with the black circle representing the region of full failure).

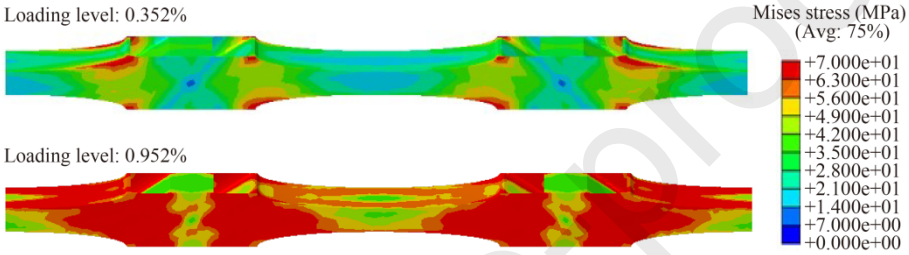

Fig. 9 Matrix damage predicted by the single layer FE model (SL-M in Table 4) evolution in warp direction, showing neat matrix only.

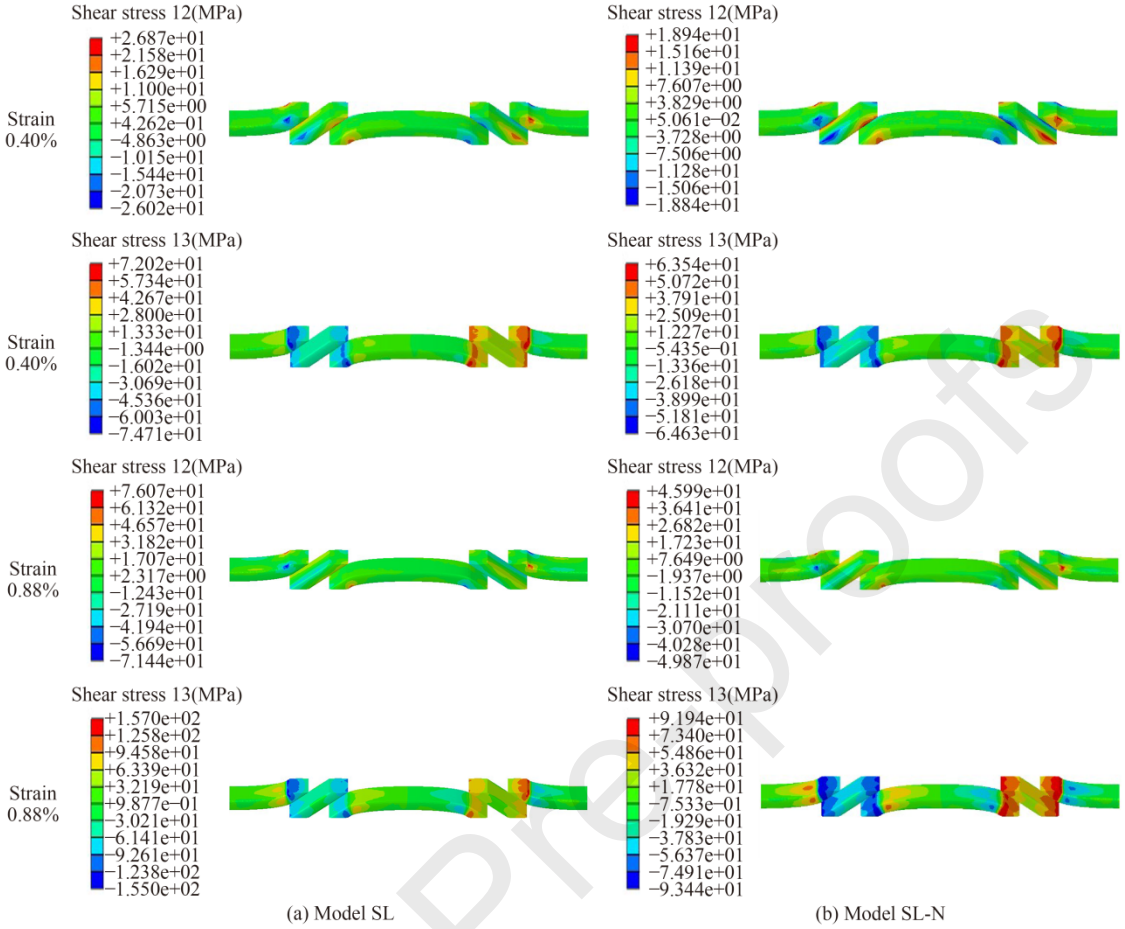

Fig. 10 Shear stress distributions (MPa) predicted by the SL (without nonlinear shear) and SL-N (with nonlinear shear) models loaded to 0.40% and 0.88% strain in warp direction, showing warp tows only.

It should be noted that all the models as have been discussed so far are based on the single layer unit cell and they overestimate the initial stiffness when compared with the experiment. The single layer unit cell was adopted in order to minimise the computational cost by assuming that there are a large enough number of layers in the thickness direction. However, for the tested composite, this assumption lacked appropriate justification. An attempt was therefore made to evaluate the possible errors this assumption as an approximation would introduce to the predicted behaviour of the material. In order to achieve this, a whole thickness model was employed as described in Section 4.4, including the surface layers of the 3D woven fabric, where the regularity breaks down in order to terminate the extent of the fabric in its thickness direction. The whole thickness model was analysed with due considerations of debonding, neat matrix damage and along fibre shear nonlinearity in the fibre tows. The obtained stress-strain curve has been plotted in Fig. 6, marked as WT. It can be seen that the initial stiffness of the whole thickness unit cell model agrees reasonably well with experiment. The disparity on the initial stiffness can therefore be attributed to the lack of representation of the finite thickness of composite and the presence of irregular fibre tow arrangement on the surfaces of the fabric preform. It can be expected that this disparity will become more pronounced as the thickness of the composite further reduces but will narrow for composites involving more layers. It will therefore be users' decision whether they can put up with the amount of error in their analysis. If so, the single layer unit cell would offer a relatively efficient means to estimate the behaviour of the composite. Otherwise, a more computationally expensive solution will have to be obtained by employing the whole thickness model.

A contour plot of the full failure on the interfaces between the fibre tows and the neat matrix is shown in Fig. 11 for the whole thickness model at a loading strain of 0.35%. Interfacial fracture as signified by hot spots, where the value of full damage variable (SDEG in Abaqus) has reached unity, shares close similarity to that predicted through the single layer model (Fig. 8), except for the surface layers which are not represented in the single layer model at all. The users may have to consider this when deciding whether to employ a single layer model or a whole thickness model in their applications. Due to the high computational costs, the responses of the whole thickness model with each of the sources of nonlinearity have not been pursued individually, but the outcomes of such exercise should not be too difficult to imagine.

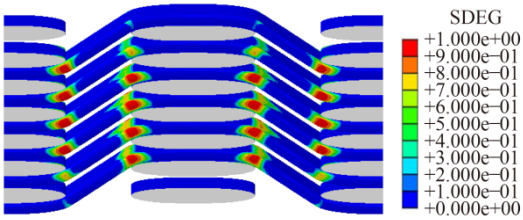

Fig. 11 Debonding damage (full failure) predicted by the whole thickness FE model with (30,30,30) MPa interfacial strengths loaded to 0.35% strain in warp direction, showing interface only.

The interfacial strengths as employed in the cohesive zone model determine the debonding damage initiation. According to the cohesive model formulation, an interface can still take further load after damage initiation until it fails completely. The values of these strengths dictate the initiation of the damage process and, to a great extent, the point when the nonlinear stress-strain curve starts to deviate from its linear path. Unfortunately, there is no established and practical means to measure the strengths of the interfaces concerned. The values employed were quoted from other publications in the literature. It is not clear how relevant these values are to the present application and how sensitive the material's responses are to the magnitudes of these values. To offer a minimal degree of evaluation, a simple parametric study based on the single layered unit cell has been conducted for three sets of these strengths, namely, (30,60,60), (30,30,30) and (15,15,15) MPa. The outcomes obtained in terms of stress-strain curves are shown in Fig. 12 allowing interfacial debonding, neat matrix damage and nonlinear shear in fibre tows. It should be noted that 15 MPa is an unusually low value for the interfacial strength in the cohesive zone model. Whilst it might be a rather conservative underestimate of properly measured values, it might bear some relevance to the problem involved in the experimental study of the particular IM7 3D woven composite, because the composite tested tended to contain a significant amount of voids as shown in Fig. 13. These voids could serve as the initiation sites, undermining the interfacial strengths to some degree. The parametric study conducted here tends to suggest the sensitivity of the overall responses of the material to the interfacial strengths in the CZM in terms of starting point, where the nonlinear stress-strain curve deviates from the linear path, and the subsequent stiffness reduction.

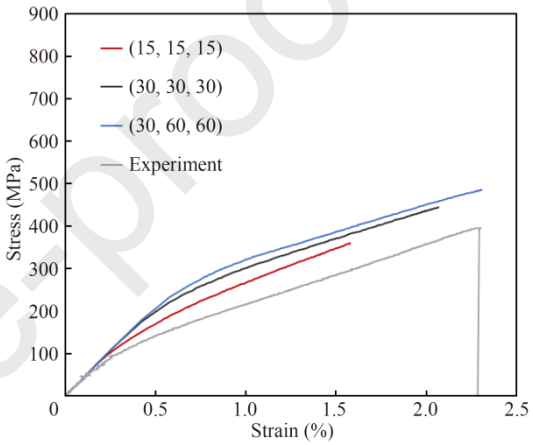

Fig. 12 Stress-strain responses from single layer (SL-MN) FE models of different interfacial strengths and experiment for the 3D woven composite in tension along the warp direction.

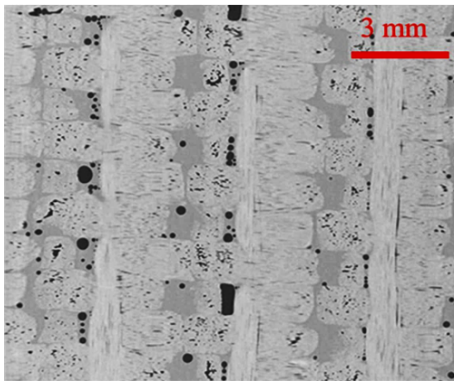

Fig. 13 Micro-CT image showing a significant amount of voids in the tested specimen.

Although the aim of this study is not to reproduce the experimental results quantitatively, the use of a set of lower interface strength (15,15,15) MPa in the

whole thickness unit cell model was attempted to demonstrate their effects on the prediction. The stress-strain curve from this model becomes closer to the experimental data due to an earlier onset of interface damage, as shown in Fig. 6 without any change in the initial stiffness, as expected. However, these lower interfacial strengths led to excessive premature damage in the model (Fig. 14) which contradicts the microscopic observation of the tested specimens. This suggests that the disparity between the predictions and the experimental data cannot be entirely attributed to the inaccurate input of the interfacial strengths.

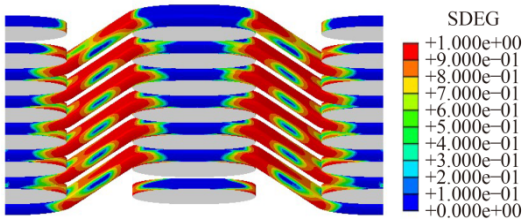

Fig. 14 Debonding damage (full failure) predicted by the whole thickness FE model with (15,15,15) MPa interfacial strengths loaded to 0.35% strain in warp direction, showing interface only.

In addition, due to the need to parameterise the generation of the unit cells, fibre architectures in the unit cells were based on the idealised topology which did not consider localised distortions caused during preform fabrication and the forming or processing stages. It is understood that this idealisation would be responsible for a degree of the discrepancies in the predicted results which will be accounted for somehow as future work in due course.

6. Conclusions

3D woven composites of a layer-to-layer angle interlock weave pattern have shown strong nonlinearity in the macroscopic constitutive response under warp direction tension testing. To efficiently use such materials in engineering applications, proper understanding of their behaviour and the capability of predicting it is imperative. In this work, various sources of nonlinearity in the finite element modelling of 3D woven composites and their modelling strategies were discussed in order to characterise this nonlinear behaviour. The investigated sources of nonlinearity include fibre tow/matrix debonding, damage in neat matrix and nonlinear shear in fibre tows. It has been demonstrated, both through the experimental means and the adopted zero-thickness cohesive element method, that the accumulation of debonding damage is partially responsible for the nonlinearity in macroscopic behaviour. In addition, damage in neat resin pocket, and nonlinear shear in fibre tows whose importance was often neglected in the previous studies, also play an important role in the nonlinear response of the studied 3D woven composites. Due to the lack of periodicity in the fibre architecture in the through-thickness direction, using a single layer of the weave topology in the unit cell model would overestimate the macroscopic stiffness even from the start of the loading. Therefore, considering the whole thickness of the weave in the unit cell is recommended if accuracy is of priority, but this will come at a price of a much higher computational cost. If the errors due to this effect can be tolerated, the single layer unit cell model remains an attractive approach, which should be suitable to use in the early design stage or in material selection when high accuracy is not the priority.

Acknowledgements

The financial support from AECC CAE, China (No.126961) is gratefully acknowledged. The HPC service at the University of Nottingham is also acknowledged. The work was also partially supported by the State Key Laboratory of Explosion Science and Technology, Beijing Institute of Technology, China(No.KFJJ9-11M) and Beihang University, China, through the 111 Centre ,China(No.B18002).

References

1. Song J, Wen WD, Cui HT. Fatigue life prediction model of 2.5D woven composites at various temperatures. *Chin J Aeronaut* 2018;**31**(2):310–29.

2. Zhao ZQ, Wei HT, Cai YL, et al. Predicting the low-velocity impact failure of 3D woven composites based on a local homogenization modeling strategy. *Compos Commun* 2024;**48**:101912.

3. Zou X, Yan SB, Matveev M, et al. Experimental and numerical investigation of interface damage in composite L-angle sections under four-point bending. *J Compos Mater* 2021;**55**(2):187-200.

4. Oddy C, Ekh M, Ekermann T, et al. A framework for macroscale modelling of inelastic deformations in 3D-woven composites. *Mech Mater* 2021;**160**:103856.

5. Mouritz AP, Cox BN. A mechanistic interpretation of the comparative in-plane mechanical properties of 3D woven, stitched and pinned composites. *Compos Part A Appl Sci Manuf* 2010;**41**(6):709–28.

6. Dahale M, Neale G, Lupicini R, et al. Effect of weave parameters on the mechanical properties of 3D woven glass composites. *Compos Struct* 2019;**223**:110947.

7. Dai S, Cunningham PR, Marshall S, et al. Influence of fibre architecture on the tensile, compressive and flexural behaviour of 3D woven composites. *Compos Part A Appl Sci Manuf* 2015;**69**:195–207.

8. Pankow M, Justusson B, Riosbaas M, et al. Effect of fiber architecture on tensile fracture of 3D woven textile composites. *Compos Struct* 2019;**225**:111139.

9. Umer R, Alhussein H, Zhou J, et al. The mechanical properties of 3D woven composites. *J Compos Mater* 2017;**51**(12):1703–16.

10. Behera BK, Dash BP. Mechanical behavior of 3D woven composites. *Mater Des* 2015;**67**:261–71.

11. Brandt J, Drechsler K, Arendts FJ. Mechanical performance of composites based on various three-dimensional woven-fibre preforms. *Compos Sci Technol* 1996;**56**(3):381–6.

12. Zhang DT, Sun MY, Liu XD, et al. Off-axis bending behaviors and failure characterization of 3D woven composites. *Compos Struct* 2019;**208**:45–55.

13. Xu MM, Sitnikova E, Li SG. Unification and parameterisation of 2D and 3D weaves and the formulation of a unit cell for composites made of such preforms. *Compos Part A Appl Sci Manuf* 2020;**133**:105868.

14. Li SG, Sitnikova E. Representative volume elements and unit cells: concepts, theory, applications and implementation. Amsterdam: Woodhead Publishing; 2020.

15. Cox BN, Dadkhah MS, Morris WL, et al. Failure mechanisms of 3D woven composites in tension, compression, and bending. *Acta Metall Mater* 1994;**42**(12):3967–84.

16. Turner P, Liu T, Zeng X. Collapse of 3D orthogonal woven carbon fibre composites under in-plane tension/compression and out-of-plane bending. *Compos Struct* 2016;**142**:286–97.

17. Kong WY. Macro-scale modelling of the impact response of 3D woven composites for aerospace applications [dissertation]. Nottingham :University of Nottingham; 2016.

18. Zhang DY, Waas AM, Yen CF. Progressive damage and failure response of hybrid 3D textile composites subjected to flexural loading, part II: Mechanics based multiscale computational modeling of progressive damage and failure. *Int J Solids Struct* 2015;**75**:321–35.

19. Liu Y, Straumit I, Vasiukov D, et al. Prediction of linear and non-linear behavior of 3D woven composite using mesoscopic voxel models reconstructed from X-ray micro-tomography. *Compos Struct* 2017;**179**:568–79.

20. Yan SB, Zeng XS, Long A. Meso-scale modelling of 3D woven composite T-joints with weave variations. *Compos Sci Technol* 2019;**171**:171–9.

21. Dhiman S, Potluri P, Silva C. Influence of binder configuration on 3D woven composites. *Compos Struct* 2015;**134**:862–8.

22. Jiao W, Chen L, Xie JB, et al. Effect of weaving structures on the geometry variations and mechanical properties of 3D LTL woven composites. *Compos Struct* 2020;**252**:112756.

23. Liu YJ, Huang CY, Xia H, et al. Research on development of 3D woven textile-reinforced composites and their flexural behavior. *Mater Des* 2021;**212**:110267.

24. Wang ZJ, Yang SY, Sun SP, et al. Multiscale modeling of mechanical behavior and failure mechanism of 3D angle-interlock woven

aluminum composites subjected to warp/weft directional tension loading. *Chin J Aeronaut* 2021;**34**(8):202–17.

25. Wang ZJ, Zhao WH, Wang F, et al. Tensile behavior and failure mechanism of 3D woven fabric reinforced aluminum composites. *Int J Mech Sci* 2023;**244**:108043.

26. Ivanov DS, Baudry F, Van Den Broucke B, et al. Failure analysis of triaxial braided composite. *Compos Sci Technol* 2009;**69**(9):1372–80.

27. Wehrkamp-Richter T, De Carvalho NV, Pinho ST. Predicting the non-linear mechanical response of triaxial braided composites. *Compos Part A Appl Sci Manuf* 2018;**114**:117–35.

28. Li YD, Yan SB, Yan Y, et al. Modelling of the compressive behavior of 3D braided tubular composites by a novel unit cell. *Compos Struct* 2022;**287**:115303.

29. Zhang WJ, Yan SB, Yan Y, et al. A parameterized unit cell model for 3D braided composites considering transverse braiding angle variation. *J Compos Mater* 2022;**56**(3):491–505.

30. Zhao XT. Multi-scale study of RTM process modelling in the manufacturing of aerospace composites [dissertation]. Nottingham: University of Nottingham; 2017.

31. Hexcel.HexTow IM7 product data [cited 2012 Dec 1]. Available from: http://www.hexcel.com.

32. Gurit .Gurit PRIMETM 20LV datasheet: Epoxy infusion system [cited 2012 Dec 1]. Available from: http://www.gurit.com.

33. Li S, Jeanmeure LFC, Pan Q. A composite material characterisation tool: UnitCells. *J Eng Math* 2015;**95**(1):279–93.

34. Yan SB, Zeng XS, Long A. Experimental assessment of the mechanical behaviour of 3D woven composite T-joints. *Compos Part B Eng* 2018;**154**:108–13.

35. Yang QD, Cox B. Cohesive models for damage evolution in laminated composites. *Int J Fract* 2005;**133**(2):107–37.

36. Barbero EJ. *Finite element analysis of composite materials using abaqus*. Boca Raton : CRC Press; 2013.

37. Harper PW, Hallett SR. Cohesive zone length in numerical simulations of composite delamination. *Eng Fract Mech* 2008;**75**(16):4774–92.

38. Li SG, Xu MM, Yan SB, et al. On the objectivity of the nonlinear along-fibre shear stress–strain relationship for unidirectionally fibre-reinforced composites. *J Eng Math* 2021;**127**(1):17.

39. Cox B, Yang QD. In quest of virtual tests for structural composites. *Science* 2006;**314**(5802):1102–7.

40. Yu TH. Continuum damage mechanics models and their applications to composite components of aero-engines [dissertation]. Nottingham : University of Nottingham; 2016.

☐ The authors declare the following financial interests/personal relationships which may be considered as potential competing interests:

Declaration of Interest Statement

☒ The authors declare that they have no known competing financial interests or personal relationships that could have appeared to influence the work reported in this paper.

☐ The author is an Editorial Board Member/Editor-in-Chief/Associate Editor/Guest Editor for this journal and was not involved in the editorial review or the decision to publish this article.